PRKN Ser131 phosphorylation promotes cigarette smoke-induced mitophagy impairment and epithelial cell senescence via MKK3/p38 MAPK activation: An *in vitro* and *in vivo* study

Yajie Hu[1+], Jianyu Liu[2*+], Mengyu Zhang[1], Jiajia Qu[1], Wenqiang Hao[1], Xinmiao Zhu[1], Dawei Wu[1], Shuo Jiang[1], Yiqing Qu[1]*

ABSTRACT

INTRODUCTION Cigarette smoke (CS) exposure impairs mitochondrial function and promotes senescence in airway epithelial cells, contributing to the pathogenesis of chronic obstructive pulmonary disease (COPD). However, the molecular mechanisms linking mitophagy dysfunction to cellular senescence remain poorly understood. Parkin (PRKN) is a key regulator of mitophagy, but whether PRKN Ser131 phosphorylation contributes to CS-induced impairment of mitophagy and senescence remains unclear. Therefore, this study aimed to investigate the role of PRKN Ser131 phosphorylation in CS-induced impairment of mitophagy and epithelial cell senescence, and to explore the underlying mechanism.

METHODS This laboratory-based experimental study utilized human bronchial epithelial BEAS-2B cells exposed to cigarette smoke extract (CSE) and a mouse model of CS-induced emphysema. Molecular interventions included mutation of PRKN at Ser131, and knockdown of mitogen-activated protein kinase kinase 3 (MKK3) to modulate the downstream p38 mitogen-activated protein kinase (p38 MAPK) pathway. Mitophagy activity, mitochondrial reactive oxygen species (ROS), and senescence markers were evaluated.

RESULTS Exposure to cigarette smoke extract (CSE) increased MKK3 expression and activated the p38 MAPK pathway, leading to phosphorylation of PRKN at Ser131. This phosphorylation was accompanied by reduced mitophagy-related readouts and increased mitochondrial ROS. Both MKK3 knockdown and modulation of mitochondrial quality-control pathways were associated with improved mitophagy-related readouts and reduced senescence markers under CSE exposure. Moreover, cells expressing the PRKN S131A mutant exhibited significantly improved mitophagy flux, reduced ROS levels, and attenuated senescence compared to wild-type PRKN. *In vivo*, emphysematous lungs showed increased MKK3 and senescence markers alongside decreased PRKN and PTEN-induced kinase 1 (PINK1) expression.

CONCLUSIONS Our findings suggest that the MKK3/p38 MAPK–PRKN Ser131 axis contributes to CS-induced mitophagy impairment and epithelial senescence. Additional studies are needed to strengthen the evidence and evaluate the translational potential of targeting this pathway in COPD.

AFFILIATION
1 Department of Pulmonary and Critical Care Medicine, Laboratory of Basic Medical Sciences, Qilu Hospital of Shandong University, Jinan, China
2 Department of Respiratory and Critical Care Medicine, Zhuzhou Central Hospital, Zhuzhou, China
*Contributed equally
+ Co-first authors

CORRESPONDENCE TO
Yiqing Qu. Department of Pulmonary and Critical Care Medicine, Laboratory of Basic Medical Sciences, Qilu Hospital of Shandong University, Wenhuaxi Road 107#, 250012, Jinan, China
E-mail: quyiqing@sdu.edu.cn
ORCID iD: https://orcid.org/0000-0002-9538-7601

KEYWORDS
chronic obstructive pulmonary disease, mitophagy, cellular senescence, MKK3, PRKN

Received: 16 November 2025
Revised: 26 February 2026
Accepted: 3 March 2026

Tob. Induc. Dis. 2026;24(May):74 https://doi.org/10.18332/tid/218816

INTRODUCTION

Chronic obstructive pulmonary disease (COPD) is a major global cause of mortality and disability, characterized by persistent respiratory symptoms and

airflow limitation that is not fully reversible, most commonly driven by long-term exposure to noxious particles and gases such as cigarette smoke[1,2]. COPD typically develops from mid-life onward and its burden increases with aging, underscoring the importance of aging-related mechanisms in disease progression[1].

Oxidative stress is a hallmark of COPD. Elevated oxidative stress biomarkers have been detected in airway-derived samples from patients with COPD, indicating a sustained oxidant burden in the diseased lung[3]. Experimentally, cigarette smoke/cigarette smoke extract (CS/CSE) increases mitochondrial reactive oxygen species (mtROS), disrupts mitochondrial homeostasis, and promotes airway epithelial senescence[4]. Because mitochondria are both a major source and a key target of ROS, persistent mtROS overload can amplify oxidative injury and downstream inflammatory signaling, including inflammasome-related pathways[5,6]. Consistent with this concept, prolonged smoke exposure alters mitochondrial structure and function in airway epithelial cells, and smoke stress promotes mitochondrial fragmentation that accompanies epithelial senescence[7,8].

Mitophagy is essential for mitochondrial quality control, and the PINK1/PRKN pathway is a canonical mechanism for selectively eliminating damaged mitochondria[9-11]. Upon mitochondrial depolarization, PINK1 accumulates on the outer mitochondrial membrane and initiates a phosphorylation cascade in which PINK1 phosphorylates PRKN and ubiquitin to promote PRKN activation and ubiquitin-dependent signaling on damaged mitochondria[12,13]. Phosphorylated ubiquitin serves as a high-affinity PRKN receptor and drives conformational activation of PRKN, thereby amplifying mitochondrial ubiquitination and recruitment of mitophagy receptors[14-16]. Downstream, the PINK1–PRKN ubiquitylation program recruits OPTN/NDP52 and activates TBK1 to execute mitophagy[17]. Consistently, Ito et al.[18] extracted lung homogenate from COPD patients and verified that the level of PRKN protein was positively associated with lung function of patients, which indicated PRKN may play a key regulatory role in the pathogenesis of COPD. Nevertheless, while cigarette smoke has been linked to impaired mitophagy and epithelial senescence, the upstream signaling events that functionally disable PRKN in COPD-relevant airway epithelial injury remain insufficiently defined[4,18].

Mitogen-activated protein kinase kinase 3 (MKK3), an upstream activator of p38 MAPK, has been implicated in mitochondrial quality control and smoke-induced inflammation. Genetic loss of MKK3 improves mitochondrial function and mitochondrial quality control and attenuates inflammatory responses in experimental lung injury and cigarette smoke exposure[19-21]. Notably, p38 MAPK has been reported to phosphorylate PRKN at Ser131, weakening PRKN function and impairing mitophagy[22]. However, whether CSE activates an MKK3/p38-dependent PRKN Ser131 phosphorylation axis to causally suppress PRKN-mediated mitophagy, thereby driving mtROS accumulation and epithelial senescence, has not been established in COPD-relevant models.

Therefore, this study aimed to determine whether cigarette smoke extract (CSE) activates the MKK3/p38 MAPK pathway to induce PRKN Ser131 phosphorylation, thereby impairing PRKN-mediated mitophagy and promoting epithelial cell senescence. We further sought to clarify the underlying mechanism using MKK3 knockdown, assessment of p38 MAPK phosphorylation/activation, and the phosphorylation-deficient PRKN S131A mutant, and to validate these findings in a CS/LPS-induced emphysema mouse model.

METHODS

Study design and reporting

This laboratory-based experimental study included *in vitro* BEAS-2B cells exposed to 5% cigarette smoke extract (CSE) and an *in vivo* CS/LPS-induced emphysema mouse model (n=7/group). Primary outcomes included mitophagy-related readouts, mitochondrial ROS, and senescence markers assessed by immunofluorescence, Western blotting, RT-qPCR, and ELISA. The animal study is reported in accordance with the ARRIVE 2.0 guidelines (Supplementary file). All experiments were conducted between January 2021 and June 2024 in China.

In vivo experiments: Animals and treatments

Male C57BL/6J mice (7 weeks old, 18–20 g) were obtained from the Animal Experimental Center of Qilu

Hospital and housed at 22 ± 2 °C, 40–60% humidity, under a 12-h light/dark cycle, with ad libitum access to food and water. Mice were acclimatized for 7 days before experiments and randomly allocated (random number method) to room-air control or cigarette smoke (CS)-exposed groups (n=7/group). For COPD induction, mice received intranasal lipopolysaccharide (LPS; 30 μg) on days 2 and 29 and were exposed to smoke from 20 cigarettes/day, 5 days/week for 1 month in a 60×57×100 cm smoking chamber; room-air controls were handled identically without CS exposure. Animals were monitored daily for general condition and signs of distress, and humane endpoints were applied according to institutional guidelines. On day 30, mice were deeply anesthetized with sodium pentobarbital, blood was collected by cardiac puncture for serum preparation, and mice were euthanized by CO2 inhalation prior to tissue harvesting. Lung tissues and bronchoalveolar lavage fluid (BALF) were collected as described above. Outcome quantification and analysis were performed blinded to group allocation. No animals were excluded from the endpoint analyses; the final numbers analyzed were n=7 per group.

In vitro experiments: Cell model

Cell culture and CSE exposure

Immortalized BEAS-2B cells (Procell Technology, Wuhan, China) within 40 passages were cultured in Dulbecco's Modified Eagle Medium (DMEM) (Gibco) supplemented with 10% fetal bovine serum (FBS) (Biological Industries) at 37°C in 5% CO_2. Cells were exposed to 5% cigarette smoke extract (CSE) for 24 h when indicated; cells cultured under identical conditions without CSE exposure served as the control group (Control/NC). Primary antibodies included β-actin (Beyotime, AF0003), glyceraldehyde-3-phosphate dehydrogenase (GAPDH) (Beyotime, AF5009), MEK3/MKK3 (Abcam, ab195037), p16 (Abcam, ab108349), p21 (CST, 2947), PINK1 (CST, 6946), Parkin (Abcam, ab77924), phospho-Parkin-Ser131 (Absci, 12371), LC3B (CST, 3868), and TOMM20 (Abcam, ab283317). Fluorescent secondary antibodies were from Beyotime or Abbkine. Mdivi-1 (GLPBIO) and Torin1 (Selleck) were used as mitophagy inhibitors and inducers, respectively.

Preparation of CSE

CSE was prepared as previously described. Mainstream smoke from one cigarette was bubbled into 10 mL of serum-free DMEM, filtered, and adjusted to pH 7.35–7.45. Absorbance at 320 nm was measured, and 100% CSE was defined as optical density at 320 nm (OD320) = 0.74 ± 0.05. CSE was diluted to working concentrations and used within 30 min.

Molecular interventions: siRNA transfection

Small interfering RNAs (siRNAs) (RiboBio) targeting MKK3 were transfected into BEAS-2B cells using Lipofectamine 2000 (Invitrogen). Knockdown efficiency was verified by RT-qPCR. The following siRNA sequences were used: negative control (si-NC, UUCUCCGAACGUGUCACGUTT) and MKK3-targeting siRNAs (si-MKK3-326, GAAGAAGGAUCUACGGAUATT; si-MKK3-612, GCACGGUCGACUGUUUCUATT; si-MKK3-994, GCUACAAUGUCAAGUCCGATT).

Molecular interventions: lentiviral infection

Lentiviral vectors overexpressing PRKN or PRKN-S131A (Genechem, Shanghai) were transduced into BEAS-2B cells. Stable lines were selected with puromycin and validated by fluorescence observation and by confirming PRKN expression at mRNA and protein levels.

Outcome measurements/assays

Western blotting

Cells were lysed in radioimmunoprecipitation assay (RIPA) buffer (Beyotime). Equal amounts of protein (10–30 μg) were resolved by 10–15% sodium dodecyl sulfate–polyacrylamide gel electrophoresis (SDS-PAGE) and transferred to polyvinylidene difluoride (PVDF) membranes (0.45 μm). Membranes were incubated with primary antibodies overnight at 4°C, followed by horseradish peroxidase (HRP)-conjugated anti-rabbit or anti-mouse secondary antibodies (CST). Bands were visualized by chemiluminescence (Tanon 4800) and quantified using ImageJ, with normalization to GAPDH.

Immunofluorescence

Cells grown on slides and treated as indicated were fixed with 4% paraformaldehyde, permeabilized with 0.03% Triton X-100, and blocked with 5% bovine

serum albumin (BSA). Primary antibodies were applied overnight at 4°C, followed by fluorescent secondary antibodies for 1 h at room temperature. Images were captured using an OLYMPUS IX81 microscope. LC3B and TOMM20 signals were merged to assess mitophagy.

RT-qPCR

Total RNA was isolated using TRIzol (Invitrogen) and reverse-transcribed with the PrimeScript RT kit (Takara). Reverse transcription quantitative polymerase chain reaction (RT-qPCR) was performed using TB Green Premix Ex Taq II (Takara). GAPDH served as an internal control. Relative mRNA expression was calculated using the $2^{-\Delta\Delta Ct}$ method.

Water-soluble tetrazolium salt-1 (WST-1) cytotoxicity assay

Cells (5×10^3/well) were seeded into 96-well plates and incubated with CSE at indicated concentrations for 24–72 h. WST-1 solution was added and mixed, and absorbance at 450 nm was recorded to assess cell viability.

ROS detection

ROS levels were detected using a dihydroethidium (DHE)-based assay kit (Beyotime). After treatment, cells were incubated with DHE and imaged by fluorescence microscopy. Fluorescence intensity was quantified with ImageJ.

Histology and immunohistochemistry

Lung tissues were processed following standard procedures. Sections were incubated with primary rabbit antibodies and HRP-conjugated secondary antibody (CST, 7074). 3,3'-diaminobenzidine (DAB) substrate (BosterBio) was used for color development.

Enzyme-linked immunosorbent assay (ELISA)

Serum samples from control and emphysema mice were collected and centrifuged at 2500g for 10 min. IL-8, TNF-α, and IL-6 levels were determined using ELISA kits (Elabscience) according to the manufacturer's instructions.

Ethical approval

All animal procedures were reviewed and approved by the Scientific Research Ethics Committee of Qilu Hospital, Shandong University (Approval No. KYLL-2022(ZM)-1062; Date: 1 November 2022) and all experiments were performed in accordance with institutional guidelines for the care and use of laboratory animals. The *in vitro* experiments were conducted using the immortalized BEAS-2B cell line purchased from a commercial supplier; this study did not involve recruitment of human participants or collection of identifiable human specimens.

Statistical analysis

Data were analyzed using SPSS 22.0 and GraphPad Prism 7.0. Results are presented as mean ± standard deviation (SD). Unless otherwise specified, *in vitro* experiments were performed with at least three independent biological replicates (n=3), and representative images are shown. Comparisons between two groups were performed using an unpaired two-tailed Student's t-test. For comparisons among three or more groups, one-way analysis of variance (ANOVA) followed by a *post hoc* multiple-comparisons test was used, as indicated in the figure legends. Normality and homogeneity of variance were assessed prior to parametric testing; when assumptions were not met, appropriate non-parametric tests were used. Western blot grayscale values were quantified using ImageJ. Differences were considered statistically significant at $p<0.05$.

RESULTS

CSE increases MKK3 and is accompanied by altered mitophagy-related readouts and increased senescence markers in BEAS-2B cells

MKK3 protein levels were higher in CSE-treated BEAS-2B cells than in untreated controls (Figure 1A). TOMM20–MAP1LC3B colocalization was reduced under CSE exposure (Figure 1B). In parallel, p16 and p21 protein levels were increased in the CSE condition (Figure 1C). To support these imaging findings at the pathway level, PINK1 and PRKN readouts under the same CSE context are provided in Supplementary file Figure S1.

MKK3 knockdown attenuates CSE-associated changes in mitophagy-related imaging readouts and reduces senescence markers across modulatory conditions

Across the indicated treatment conditions, TOMM20–

Figure 1. CSE exposure increases MKK3 and is accompanied by reduced TOMM20–MAP1LC3B colocalization and increased senescence markers in BEAS-2B cells (5% CSE, 24 h; n=3): A) Representative immunoblot of mitogen-activated protein kinase kinase 3 (MKK3) in BEAS-2B cells in the negative control (NC) and 5% cigarette smoke extract (CSE) groups, with densitometric quantification normalized to glyceraldehyde-3-phosphate dehydrogenase (GAPDH); B) Representative immunofluorescence images (200×) showing translocase of outer mitochondrial membrane 20 (TOMM20) and microtubule-associated proteins 1A/1B light chain 3B (MAP1LC3B/LC3B), and merged images, in the indicated groups; C) Representative immunoblots of cyclin-dependent kinase inhibitor 2A (p16/CDKN2A) and cyclin-dependent kinase inhibitor 1A (p21/CDKN1A) with densitometric quantification normalized to GAPDH

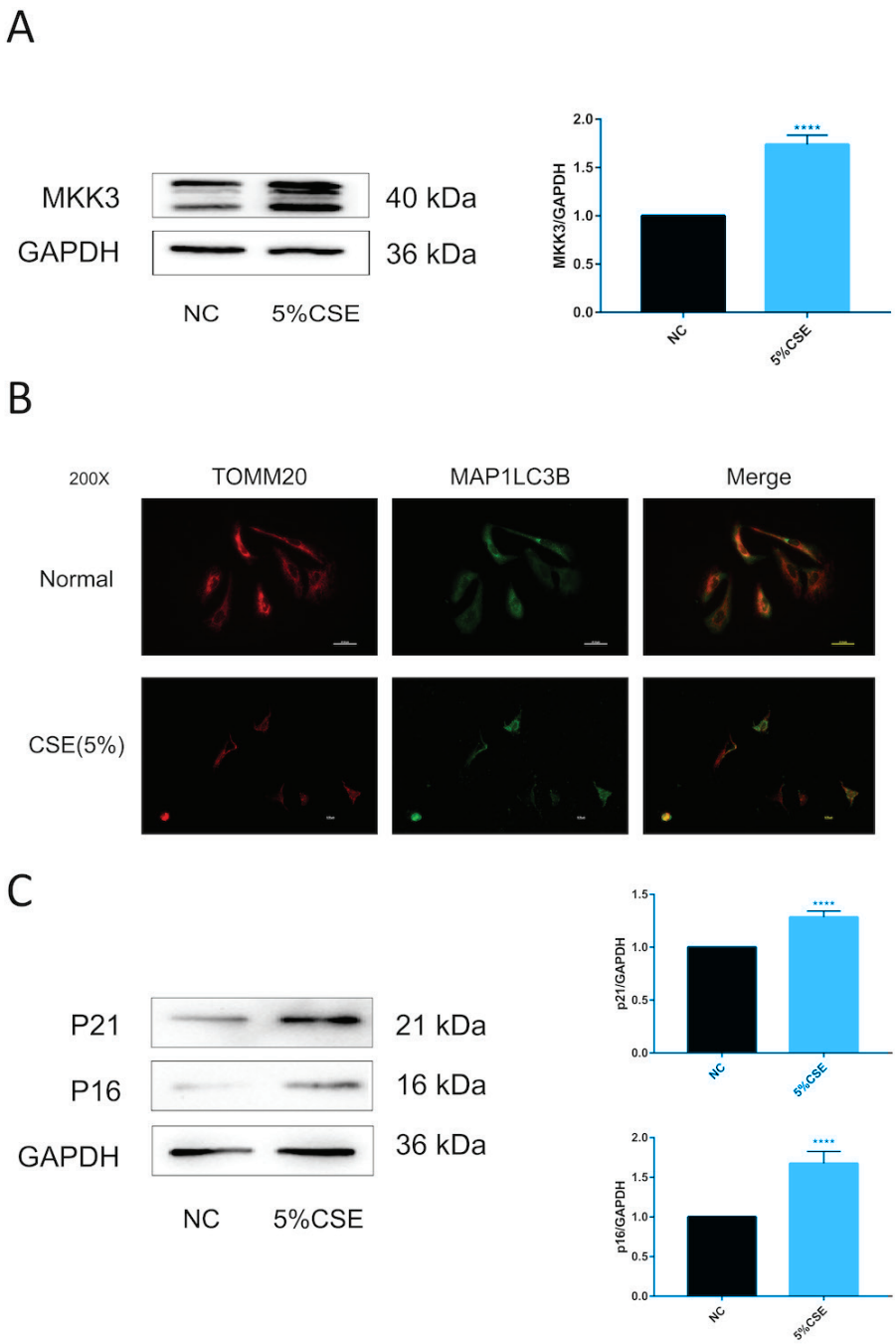

Data are presented as mean ± SD from n=3 independent biological replicates. For immunoblot quantification, values are shown as relative protein levels (normalized to GAPDH; arbitrary units). Horizontal brackets indicate the groups compared. Statistical analysis: two-tailed unpaired Student's t-test (two-group comparisons). *p<0.05, **p<0.01, ***p<0.001, ****p<0.0001. ns: not significant.

Figure 2. MKK3 knockdown is associated with improved TOMM20–MAP1LC3B colocalization and reduced senescence markers under CSE exposure with modulatory conditions (5% CSE, 24 h; n=3): A) Representative immunofluorescence images (200×) of TOMM20, MAP1LC3B (LC3B), and merged images in the following groups: Normal, 5% CSE, 5% CSE + siMKK3, 5% CSE + siNC, 5% CSE + Torin1, and 5% CSE + siMKK3 + Mdivi1; B) Representative immunoblots of p16 and p21 with densitometric quantification normalized to GAPDH across the indicated groups

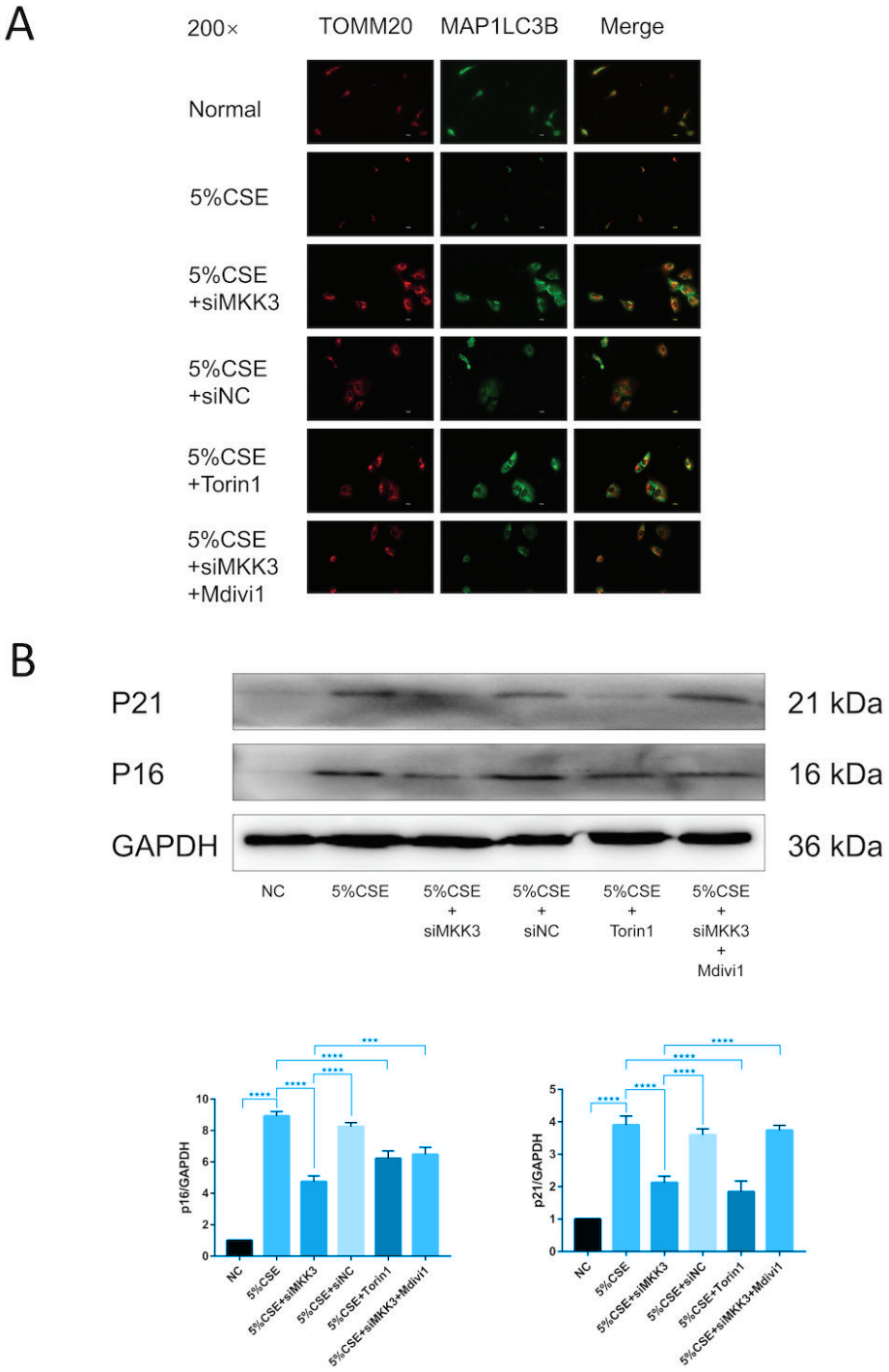

Data are presented as mean ± SD from n=3 independent biological replicates. Immunoblot quantification is shown as relative protein levels (normalized to GAPDH; arbitrary units). Horizontal brackets indicate the groups compared. Statistical analysis: one-way ANOVA with post hoc multiple-comparisons test for multi-group comparisons (as shown). siMKK3: MKK3-targeting small interfering RNA. siNC: negative-control siRNA. Torin1: mTOR inhibitor. Mdivi1: mitochondrial division inhibitor 1. **p<0.01, ***p<0.001, ****p<0.0001. ns: not significant.

Figure 3. MKK3 knockdown is associated with reduced p38 MAPK phosphorylation and reduced PRKN Ser131 phosphorylation under CSE exposure (5% CSE, 24 h; n=3):
A) Representative immunoblots and densitometric quantification of phosphorylated p38 MAPK (p-p38 MAPK) and total p38 MAPK in the indicated groups, with quantification shown as relative intensity normalized to GAPDH; B) Representative immunoblot and densitometric quantification of PRKN (Parkin) phosphorylated at Ser131 (p-S131-PRKN) in the indicated groups, normalized to GAPDH

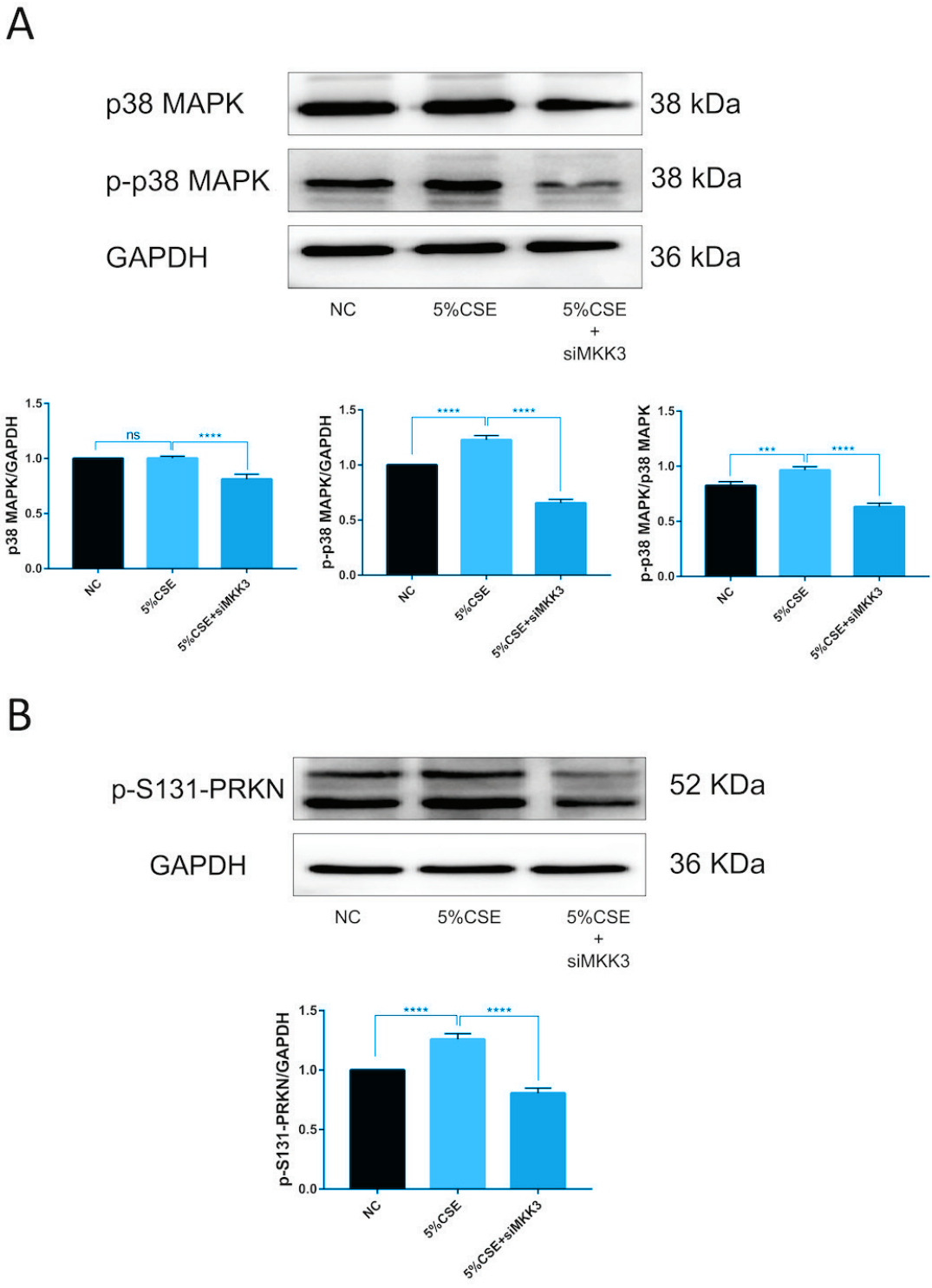

Data are presented as mean ± SD from n=3 independent biological replicates. Horizontal brackets indicate the groups compared. Statistical analysis: one-way ANOVA with post hoc multiple-comparisons test or two-tailed unpaired Student's t-test, as appropriate for the displayed comparisons. **p<0.01, ***p<0.001, ****p<0.0001. ns: not significant.

Figure 4. Emphysema mouse lungs show increased MKK3 and senescence markers and reduced PINK1/PRKN levels (20 cigarettes/day, 5 days/week, 1 month; n=7 mice/group): Representative immunoblots and densitometric quantification of PTEN-induced kinase 1 (PINK1), PRKN (Parkin), MKK3, p16 (CDKN2A), and p21 (CDKN1A) in lung tissues from control and emphysema mice, normalized to GAPDH

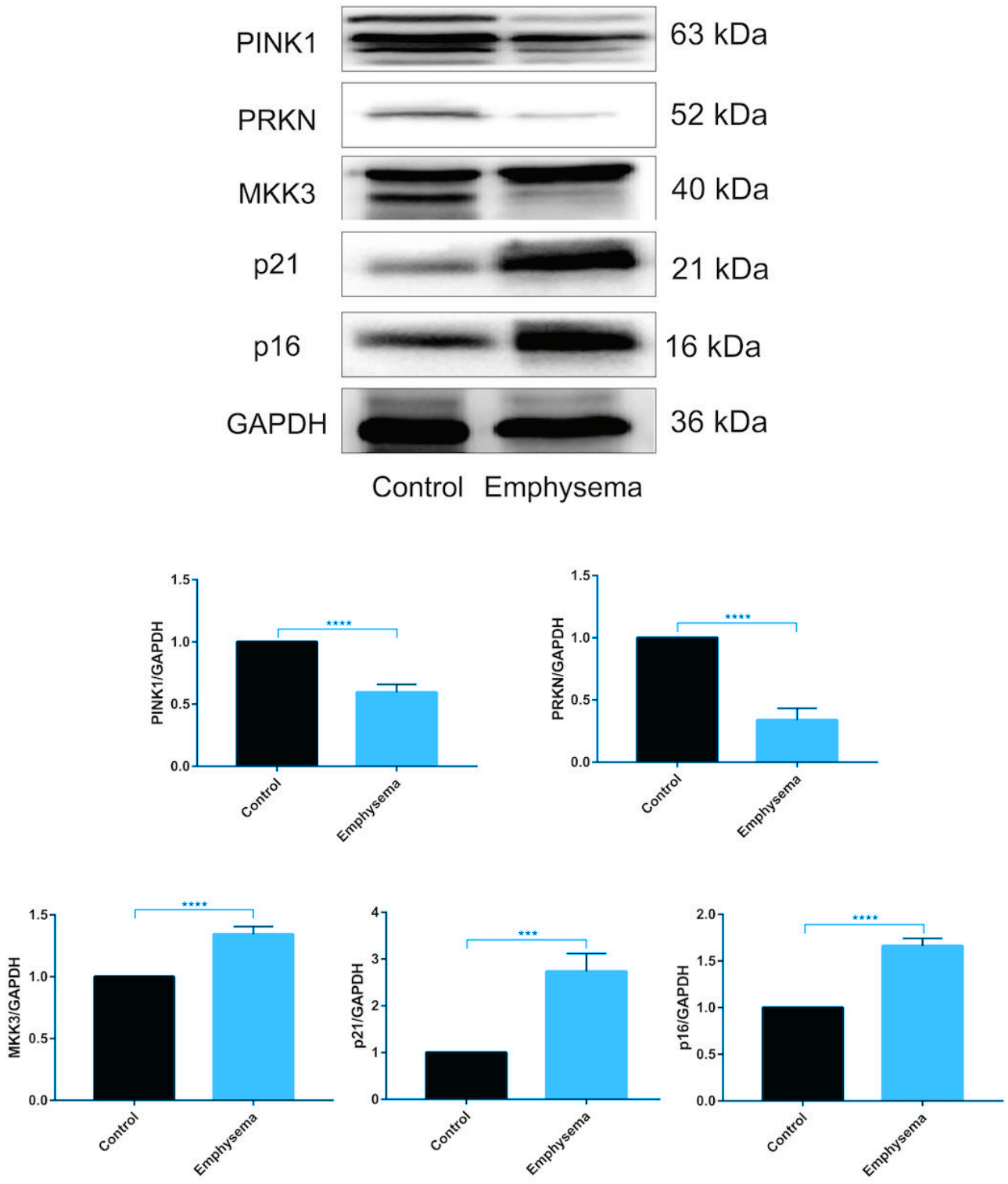

Data are presented as mean ± SD; n=7 mice per group. Immunoblot quantification is shown as relative protein levels (normalized to GAPDH; arbitrary units). Statistical analysis: two-tailed unpaired Student's t-test. **p<0.01, ***p<0.001, ****p<0.0001. ns: not significant.

MAP1LC3B colocalization was higher in the siMKK3 condition than in the CSE condition (Figure 2A). Under the same experimental framework, p16 and p21 protein levels were lower in the siMKK3 condition than in the CSE condition (Figure 2B). The efficiency of MKK3 silencing and siRNA-related validation is shown in Supplementary file Figure S2. In addition, PINK1/PRKN molecular readouts across the corresponding conditions are provided in Supplementary file Figure S3.

MKK3 knockdown is associated with reduced p38 MAPK phosphorylation and reduced PRKN Ser131 phosphorylation

p38 MAPK phosphorylation was increased under CSE exposure, whereas total p38 MAPK levels were comparatively stable (Figure 3A). p38 MAPK phosphorylation was lower in the siMKK3 condition than in the CSE condition (Figure 3A). PRKN Ser131 phosphorylation (p-S131-PRKN) was increased under CSE exposure and was reduced in the siMKK3 condition (Figure 3B). Additional supporting blots and related validation panels are included in the supplementary dataset as part of the figure set (see Supplementary file Figure S2 for knockdown validation and Supplementary file Figure S3 for pathway-level readouts under matched conditions).

Emphysema mouse lungs show concordant changes in MKK3, PINK1/PRKN, and senescence markers

In emphysema mouse lungs, MKK3, p16, and p21 levels were higher than in controls, whereas PINK1 and PRKN levels were lower (Figure 4). Histological evidence and inflammatory-marker measurements supporting the emphysema model are provided in Supplementary file Figure S4.

PRKN manipulation: construct validation and extended readouts under PRKN overexpression and PRKN S131A

PRKN overexpression and PRKN S131A expression are validated at the protein and mRNA levels in Supplementary file Figure S5. Under CSE exposure, TOMM20–MAP1LC3B colocalization and ROS-related imaging readouts under PRKN manipulation are provided in Supplementary file Figure S6, and senescence-marker measurements under extended conditions (including modulatory treatment) are shown in Supplementary file Figure S7.

DISCUSSION

In this study, we identify MKK3 as a key factor associated with cigarette smoke-induced disruption of mitochondrial quality control in airway epithelial cells. CSE exposure increased MKK3 expression and was accompanied by enhanced p38 MAPK phosphorylation and PRKN Ser131 phosphorylation, together with reduced PRKN/PINK1-related mitophagy readouts and increased senescence markers. Moreover, suppression of the p38 MAPK pathway via MKK3 silencing attenuated these changes, and expression of the phosphorylation-deficient PRKN S131A mutant further supported the functional relevance of Ser131 phosphorylation. Below, we discuss these findings in the context of prior literature and their potential implications for COPD pathogenesis.

Clinical and experimental studies have demonstrated that COPD patients exhibit marked mitochondrial dysfunction[23,24]. Mitochondria are highly sensitive to oxidative stress; under physiological conditions, mitochondrial ROS act as second messengers to maintain intracellular homeostasis[25]. Excess ROS damages mitochondrial DNA (mtDNA)[26], alters electron transport efficiency, and promotes further ROS accumulation, forming a vicious cycle. Persistent cigarette smoke exposure produces high ROS levels and leads to mitochondrial structural abnormalities, including loss of cristae, swelling, and fragmentation, consistent with observations in airway epithelial cells from COPD patients[27]. These changes are associated with decreased oxygen consumption, ATP production, mitochondrial membrane potential, and electron transport chain activity. Excess mtROS can further trigger inflammation via tumor necrosis factor receptor (TNFR), MAPK, and NLR family pyrin domain containing 3 (NLRP3) signaling pathways.

Mitophagy – particularly the PINK1/PRKN pathway – is a central mechanism of mitochondrial quality control. Loss of PINK1 or PRKN enhances inflammation, activates the cGAS–STING (cyclic GMP–AMP synthase–stimulator of interferon genes) pathway, and increases interleukin-1 beta (IL-1β) secretion[28]. Patients with PRKN/PINK1

mutations exhibit elevated interleukin-6 (IL-6) and circulating cell-free mtDNA[29], highlighting the link between impaired mitophagy and inflammation-related diseases. Cellular senescence, another major COPD phenotype, is also driven by mitochondrial dysfunction[30], telomere damage, and accumulated mtDNA mutations[31,32]. PRKN dysfunction accelerates aging phenotypes and shortens lifespan, whereas its overexpression exerts protective effects[33]. Previous studies associated CS exposure with impaired mitophagy and increased senescence in airway epithelial cells. Ito et al.[18] showed that ROS accumulation impairs mitophagy and drives senescence, while Hara et al.[8] demonstrated that PRKN is a rate-limiting factor in CS-induced mitophagy.

In this context, we confirmed that CSE increased MKK3 levels and impaired mitophagy in BEAS-2B cells, accompanied by reduced PINK1/PRKN proteins and decreased LC3 puncta. Senescence markers p16 and p21 were elevated, supporting that CSE induces mitochondrial dysfunction and senescence. Silencing MKK3 effectively restored mitophagy and alleviated senescence. Although the transfection reagent Lipofectamine 2000 increased LC3 fluorescence in si-NC cells, the fluorescence was diffuse with poor colocalization and did not reduce p16/p21 to the same extent as MKK3 knockdown. These findings indicate that the protective effects observed following MKK3 inhibition are independent of Lipo3000 and mediated through enhanced mitophagy. Rescue experiments using Mdivi1 further confirmed that restored mitophagy is required for the anti-senescence effects of MKK3 inhibition.

Mechanistically, MKK3 is known to activate p38 MAPK, a kinase involved in mitochondrial dysfunction. In Parkinson's disease, α-synuclein A53T activates p38 MAPK, which phosphorylates PRKN at Ser131 and compromises its function. Consistent with this, our results showed that CSE-induced up-regulation of MKK3 increased p38 MAPK phosphorylation and PRKN Ser131 phosphorylation, while MKK3 knockdown reversed both. To validate the functional significance of Ser131, we introduced a PRKN S131A mutant via lentiviral vectors. PRKN S131A most effectively restored mitophagy, reduced mitochondrial ROS, and attenuated senescence compared with wild-type PRKN, confirming Ser131 as a critical damage site for MKK3-p38 signaling.

Recent studies have expanded the regulatory network of PRKN-dependent mitophagy. PRKN can be modulated via protein kinase A (PKA)-p38-cAMP response element-binding protein (CREB), deubiquitination by ubiquitin-specific protease 33 (USP33), and microRNA regulation such as miR-218[34]. PRKN-independent pathways (BNIP3L, BNIP3, FUNDC1, FKBP8, BCL2L13, AMBRA1, PHB2, cardiolipin, ceramide) further emphasize the complexity of mitochondrial quality control[35].

In vivo, our mouse model with CS plus LPS reproduced emphysematous lesions and increased inflammatory cytokines. Lung tissues showed elevated MKK3, p16, and p21, with reduced PINK1/PRKN, indicating impaired mitophagy and intensified senescence. Although previous studies suggested that PINK1-/- mice are resistant to CS-induced emphysema, this discrepancy may reflect differences in modeling strategies or tissue contexts. Further validation using human COPD samples is warranted.

Limitations

This study has several limitations. First, our conclusions are based on laboratory models, including BEAS-2B cells exposed to cigarette smoke extract and a CS/LPS-induced emphysema mouse model; therefore, the generalizability to human COPD requires further validation in clinical samples. Second, the *in vitro* system relies on a single immortalized bronchial epithelial cell line and an acute CSE exposure paradigm, which may not fully recapitulate the cellular heterogeneity, chronic exposure patterns, and microenvironmental interactions present in human airways. Third, while our data support involvement of the MKK3/p38 MAPK–PRKN Ser131 pathway in mitophagy impairment and senescence, additional studies using primary human airway epithelial cells and further *in vivo* validation will be important to strengthen the evidence base and translational relevance.

CONCLUSIONS

Our findings support a model in which cigarette smoke exposure is associated with MKK3/p38 MAPK activation and PRKN Ser131 phosphorylation,

accompanied by impaired PRKN-dependent mitophagy and increased epithelial senescence markers *in vitro* and *in vivo*. These findings highlight the MKK3–p38 MAPK–PRKN pathway as a mechanistic link between cigarette smoke exposure, mitophagy disruption, and epithelial senescence in COPD. Further studies, particularly in primary human samples and additional *in vivo* models, are needed to strengthen the evidence and define the translational relevance of this pathway.

REFERENCES

1. GBD 2021 Causes of Death Collaborators. Global burden of 288 causes of death and life expectancy decomposition in 204 countries and territories and 811 subnational locations, 1990-2021: A systematic analysis for the Global Burden of Disease Study 2021. Lancet. 2024;403(10440):2100-2132. doi:10.1016/S0140-6736(24)00367-2
2. Agustí A, Celli BR, Criner GJ, et al. Global Initiative for Chronic Obstructive Lung Disease 2023 Report: GOLD executive summary. Am J Respir Crit Care Med. 2023;207(7):819-837. doi:10.1164/rccm.202301-0106PP
3. Barnes PJ. Oxidative stress in chronic obstructive pulmonary disease. Antioxidants (Basel). 2022;11(5):965. doi:10.3390/antiox11050965
4. Ahmad T, Sundar IK, Lerner CA, et al. Impaired mitophagy leads to cigarette smoke stress-induced cellular senescence: Implications for chronic obstructive pulmonary disease. FASEB J. 2015;29(7):2912-2929. doi:10.1096/fj.14-268276
5. Zorov DB, Juhaszova M, Sollott SJ. Mitochondrial reactive oxygen species (ROS) and ROS-induced ROS release. Physiol Rev. 2014;94(3):909-950. doi:10.1152/physrev.00026.2013
6. Minutoli L, Puzzolo D, Rinaldi M, et al. ROS-mediated NLRP3 inflammasome activation in brain, heart, kidney, and testis ischemia/reperfusion injury. Oxid Med Cell Longev. 2016;2016:2183026. doi:10.1155/2016/2183026
7. Hoffmann RF, Zarrintan S, Brandenburg SM, et al. Prolonged cigarette smoke exposure alters mitochondrial structure and function in airway epithelial cells. Respir Res. 2013;14(1):97. doi:10.1186/1465-9921-14-97
8. Hara H, Araya J, Ito S, et al. Mitochondrial fragmentation in cigarette smoke-induced bronchial epithelial cell senescence. Am J Physiol Lung Cell Mol Physiol. 2013;305(10):L737-L746. doi:10.1152/ajplung.00146.2013
9. Youle RJ, Narendra DP. Mechanisms of mitophagy. Nat Rev Mol Cell Biol. 2011;12(1):9-14. doi:10.1038/nrm3028
10. Matsuda N, Sato S, Shiba K, et al. PINK1 stabilized by mitochondrial depolarization recruits Parkin to damaged mitochondria and activates latent Parkin for mitophagy. J Cell Biol. 2010;189(2):211-221. doi:10.1083/jcb.200910140
11. Narendra DP, Jin SM, Tanaka A, et al. PINK1 is selectively stabilized on impaired mitochondria to activate Parkin. PLoS Biol. 2010;8(1):e1000298. doi:10.1371/journal.pbio.1000298
12. Kondapalli C, Kazlauskaite A, Zhang N, et al. PINK1 is activated by mitochondrial membrane potential depolarization and stimulates Parkin E3 ligase activity by phosphorylating Serine 65. Open Biol. 2012;2(5):120080. doi:10.1098/rsob.120080
13. Koyano F, Okatsu K, Kosako H, et al. Ubiquitin is phosphorylated by PINK1 to activate parkin. Nature. 2014;510(7503):162-166. doi:10.1038/nature13392
14. Kazlauskaite A, Martínez-Torres RJ, Wilkie S, et al. Binding to serine 65-phosphorylated ubiquitin primes Parkin for optimal PINK1-dependent phosphorylation and activation. EMBO Rep. 2015;16(8):939-954. doi:10.15252/embr.201540352
15. Okatsu K, Koyano F, Kimura M, et al. Phosphorylated ubiquitin chain is the genuine Parkin receptor. J Cell Biol. 2015;209(1):111-128. doi:10.1083/jcb.201410050
16. Wauer T, Simicek M, Schubert A, Komander D. Mechanism of phospho-ubiquitin-induced PARKIN activation. Nature. 2015;524(7565):370-374. doi:10.1038/nature14879
17. Heo JM, Ordureau A, Paulo JA, Rinehart J, Harper JW. The PINK1-PARKIN mitochondrial ubiquitylation pathway drives a program of OPTN/NDP52 recruitment and TBK1 activation to promote mitophagy. Mol Cell. 2015;60(1):7-20. doi:10.1016/j.molcel.2015.08.016
18. Ito S, Araya J, Kurita Y, et al. PARK2-mediated mitophagy is involved in regulation of HBEC senescence in COPD pathogenesis. Autophagy. 2015;11(3):547-559. doi:10.1080/15548627.2015.1017190
19. Mannam P, Shinn AS, Srivastava A, et al. MKK3 regulates mitochondrial biogenesis and mitophagy in sepsis-induced lung injury. Am J Physiol Lung Cell Mol Physiol. 2014;306(7):L604-L619. doi:10.1152/ajplung.00272.2013
20. Srivastava A, McGinniss J, Wong Y, et al. MKK3 deletion improves mitochondrial quality. Free Radic Biol Med. 2015;87:373-384. doi:10.1016/j.freeradbiomed.2015.06.024
21. Mannam P, Rauniyar N, Lam TT, Luo R, Lee PJ, Srivastava A. MKK3 influences mitophagy and is involved in cigarette smoke-induced inflammation. Free Radic Biol Med. 2016;101:102-115. doi:10.1016/j.freeradbiomed.2016.10.001
22. Chen J, Ren Y, Gui C, et al. Phosphorylation of Parkin at serine 131 by p38 MAPK promotes mitochondrial dysfunction and neuronal death in mutant A53T α-synuclein model of Parkinson's disease. Cell Death Dis. 2018;9(6):700. doi:10.1038/s41419-018-0722-7
23. Mizumura K, Cloonan SM, Nakahira K, et al. Mitophagy-dependent necroptosis contributes to the pathogenesis of COPD. J Clin Invest. 2014;124(9):3987-4003. doi:10.1172/JCI74985
24. Malinska D, Szymański J, Patalas-Krawczyk P, et al. Assessment of mitochondrial function following short- and long-term exposure of human bronchial epithelial cells

to total particulate matter from a candidate modified-risk tobacco product and reference cigarettes. Food Chem Toxicol. 2018;115:1-12. doi:10.1016/j.fct.2018.02.013
25. Yakes FM, Van Houten B. Mitochondrial DNA damage is more extensive and persists longer than nuclear DNA damage in human cells following oxidative stress. Proc Natl Acad Sci U S A. 1997;94(2):514-519. doi:10.1073/pnas.94.2.514
26. Kujoth GC, Hiona A, Pugh TD, et al. Mitochondrial DNA mutations, oxidative stress, and apoptosis in mammalian aging. Science. 2005;309(5733):481-484. doi:10.1126/science.1112125
27. Hoffmann RF, Jonker MR, Brandenburg SM, et al. Mitochondrial dysfunction increases pro-inflammatory cytokine production and impairs repair and corticosteroid responsiveness in lung epithelium. Sci Rep. 2019;9(1):15047. doi:10.1038/s41598-019-51517-x
28. Sliter DA, Martinez J, Hao L, et al. Parkin and PINK1 mitigate STING-induced inflammation. Nature. 2018;561(7722):258-262. doi:10.1038/s41586-018-0448-9. Retracted in: Nature. 2025;644(8078):1116. doi:10.1038/s41586-025-09346-8
29. Jang JY, Blum A, Liu J, Finkel T. The role of mitochondria in aging. J Clin Invest. 2018;128(9):3662-3670. doi:10.1172/JCI120842
30. Birch J, Barnes PJ, Passos JF. Mitochondria, telomeres and cell senescence: Implications for lung ageing and disease. Pharmacol Ther. 2018;183:34-49. doi:10.1016/j.pharmthera.2017.10.005
31. Trifunovic A, Wredenberg A, Falkenberg M, et al. Premature ageing in mice expressing defective mitochondrial DNA polymerase. Nature. 2004;429(6990):417-423. doi:10.1038/nature02517
32. Rana A, Rera M, Walker DW. Parkin overexpression during aging reduces proteotoxicity, alters mitochondrial dynamics, and extends lifespan. Proc Natl Acad Sci U S A. 2013;110(21):8638-8643. doi:10.1073/pnas.1216197110
33. Yao H, Chung S, Hwang JW, et al. SIRT1 protects against emphysema via FOXO3-mediated reduction of premature senescence in mice. J Clin Invest. 2012;122(6):2032-2045. doi:10.1172/JCI60132
34. Di Rita A, Maiorino T, Bruqi K, Volpicelli F, Bellenchi GC, Strappazzon F. miR-218 inhibits mitochondrial clearance by targeting PRKN E3 Ubiquitin Ligase. Int J Mol Sci. 2020;21(1):355. doi:10.3390/ijms21010355
35. Terešak P, Lapao A, Subic N, Boya P, Elazar Z, Simonsen A. Regulation of PRKN-independent mitophagy. Autophagy. 2022;18(1):24-39. doi:10.1080/15548627.2021.1888244

ACKNOWLEDGEMENTS
We appreciate all the people involved in this study.

CONFLICTS OF INTEREST
The authors have each completed and submitted an ICMJE form for disclosure of potential conflicts of interest. The authors declare that they have no competing interests, financial or otherwise, related to the current work. All authors report that since the initial planning of the work received support from the Natural Science Foundation of Shandong Province (Grant No. ZR2023QH397), the National Natural Science Foundation of China – Major Project (Grant No. 72293582) and the ECCM Program of Clinical Research Center of Shandong University (Grant No. 2021SDUCRCB001). Payments were made to their institutions.

FUNDING
The work was supported by the Natural Science Foundation of Shandong Province (Grant No. ZR2023QH397), the Major Project of National Natural Science Foundation of China (Grant No. 72293582) and the ECCM Program of Clinical Research Center of Shandong University (Grant No.2021SDUCRCB001).

ETHICAL APPROVAL AND INFORMED CONSENT
All animal procedures were reviewed and approved by the Scientific Research Ethics Committee of Qilu Hospital, Shandong University (Approval No. KYLL-2022(ZM)-1062; Date: 1 November 2022) and all experiments were performed in accordance with institutional guidelines for the care and use of laboratory animals. Additionally, the completed ARRIVE checklist for reporting animal research, can be found in the Supplementary file.

DATA AVAILABILITY
The data supporting this research are available from the authors on reasonable request.

AUTHORS' CONTRIBUTIONS
YH and JL: research concept and design. YH, JL, MZh and SJ: collection and/or assembly of data. YH, JL, JQ, WH, XZ and DW: data analysis and interpretation. YH and YQ: writing and reviewing of the manuscript. JL and MZh: writing of the manuscript. JQ and WH: reviewing of the manuscript. YQ: conceptualization, funding acquisition, supervision, editing of the manuscript. All authors read and approved the final version of the manuscript.

PROVENANCE AND PEER REVIEW
Not commissioned; externally peer reviewed.